JOC The Journal of Organic Chemistry

Article

Peptoid helix displaying flavone and porphyrin: Synthesis and intramolecular energy transfer

Woojin Yang, Junhyuk Jo, Hyeongyeol Oh, Hohjai Lee, Won-jin Chung, and Jiwon Seo

J. Org. Chem., **Just Accepted Manuscript** • DOI: 10.1021/acs.joc.9b02358 • Publication Date (Web): 28 Oct 2019

is published by the American Chemical Society. 1155 Sixteenth Street N.W., Washington, DC 20036

Peptoid helix displaying flavone and porphyrin: Synthesis and intramolecular energy transfer

Woojin Yang,† Junhyuk Jo,† Hyeongyeol Oh,† Hohjai Lee,* Won-jin Chung,* Jiwon Seo*

Department of Chemistry, School of Physics and Chemistry, Gwangju Institute of Science and Technology, 123 Cheomdan-gwagiro, Buk-gu, Gwangju 61005, South Korea.

* Corresponding authors

Email: jseo@gist.ac.kr (J. Seo), wjchung@gist.ac.kr (W.-j. Chung), and hohjai@gist.ac.kr (H. Lee)

† These authors contributed equally to this work.

Abstract

Natural light-harvesting complexes (LHCs) absorb a broad spectrum of sunlight using a collection of photosynthetic pigments whose spatial arrangement is controlled by a protein matrix and exhibit efficient energy transfer. We constructed a novel light-harvesting protein mimic, which absorbs light in the UV to visible region (280−700 nm) by displaying flavone and porphyrin on a peptoid helix. First, an efficient synthesis of 4'-derivatized 7-methoxyflavone (7-MF, **3** and **4**) was developed. The flavone-porphyrin-peptoid conjugate (FPPC) was then prepared via Miyaura borylation on a resin-bound peptoid followed by Suzuki coupling between the peptoid and pigment. Circular dichroism spectroscopy indicated that the FPPC underwent helix-to-loop conversion of the peptoid scaffold upon changing the solvent conditions. A distinct intramolecular energy transfer was observed from 7-MF to porphyrin with greater efficiency in the helix than that in the loop conformation of the peptoid, while no clear evidence of energy transfer was obtained for unstructured FPPC. We thus demonstrate the value of the helical peptoid, which provided a controlled orientation for 7-MF and porphyrin and modulated the energy transfer efficiency via conformational switching. Our work provides a way to construct a sophisticated LHC mimic with enhanced coverage of the solar spectrum and controllable energy transfer efficiency.

Introduction

Light harvesting is the first step in natural photosynthesis. Photosynthetic antenna proteins, often called light-harvesting complexes (LHCs), absorb incoming photons and transfer light energy to reaction centers, which generate excited electrons and oxidize water molecules. LHCs are composed of a spatial arrangement of photosynthetic pigments such as chlorophylls, carotenoids, and flavonoids, which absorb blue/red, green, and ultraviolet light, respectively, covering most of the sunlight available.[1] Inspired by natural photosynthetic proteins, artificial LHCs have been constructed on various scaffolds (e.g., peptides and DNA) displaying porphyrins and carotenoids.[2–5] However, the flavonoids have been rarely utilized for this purpose.

Flavonoids perform multiple roles in plants.[6] As the origin of their name suggests (from the Latin word *flavus*, which means yellow), flavonoids are pigments found in flowers and fruits,[7] but more importantly they are phytoprotective substances against ultraviolet light (i.e., UV-B, 280–315 nm) or oxidative damage.[8–10] The function of flavonoids further encompasses detoxification,[11] signaling,[12] and antimicrobial activity.[13]

Flavones have diverse molecular structures and properties. The basic skeleton of the flavones consists of three parts: Two phenyl rings (ring A and B) and one 4-pyrone ring (ring C) (compound **4**, Scheme 1).[14] The photophysical and chemical properties of the flavones can be readily modulated by hydroxylation or methoxylation.[15–17] Specifically, their light absorption spectrum shifts toward the red light region when the number of oxygen substituents is increased.[17] Self-association of these flavonoids modulates their optical and electronic characteristics as well: a phenomenon known as copigmentation occurs via non-covalent interactions such as π–π stacking, hydrophobic interaction, or hydrogen bonding.[18] Alternatively, the properties of the flavonoids can be altered upon conjugation with other

molecules. For example, conjugates with phthalocyanine,[19] fullerene,[20] and paclitaxel[21] have been reported, which lead to distinct spectroscopic, antioxidant, and cytotoxic properties, respectively.

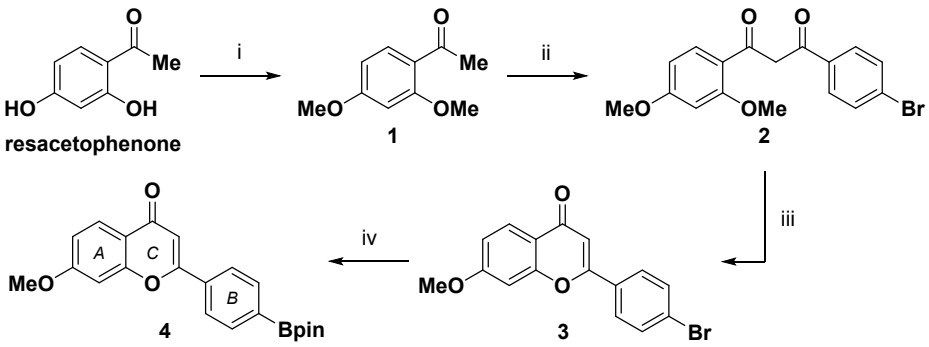

Scheme 1. Synthesis of 7-methoxyflavone derivatives **3** and **4**. Reaction conditions: (i) MeI, K_2CO_3, 94%; (ii) NaHMDS, methyl 4-bromobenzoate, 63%; (iii) 48% HBr (aq), NaI, AcOH, 55%; (iv) B_2pin_2, $PdCl_2(dppf)$, KOAc, 50%.

Attempts to conjugate flavonoids with porphyrin, a synthetic analog of the photosynthetic pigment chlorophyll, have been reported.[22–23] Cavaleiro and coworkers synthesized flavone-porphyrin dyads employing either 1,3-dipolar cycloaddition[22] or Buchwald-Hartwig amination[23] reactions. Considering their use in photodynamic therapy applications, the photophysical properties of the flavone-porphyrin dyads were evaluated, and the coupling of the flavone to porphyrin led to either increased or decreased quantum yields depending on the position of the flavone linkage or the presence of a porphyrin core metal. During an energy transfer study, Song and coworkers conjugated coumarin to porphyrin and demonstrated that the spectral overlap between the emission of coumarin and the absorption of porphyrin directly affects the intramolecular energy transfer efficiency in the complex.[24] More recently, Gust and coworkers constructed a hexad from four coumarins and two zinc porphyrins, in which zinc metal was used as a coordination site to connect an electron-accepting fullerene molecule.[25] The artificial coumarin–porphyrin–fullerene system displayed energy transfer between the

coumarin and porphyrin moieties, followed by photoinduced electron transfer from the pigments to fullerene, mimicking the natural photosynthetic reaction center. Coumarin can be considered as a simplified form of the flavonoids, where the peripheral phenyl ring of the flavone (ring B) is removed. Unlike coumarin, natural flavonoids (e.g., 7-methoxyflavone) have been rarely reported for the construction of artificial light-harvesting systems due to the lack of established conjugation methods involving the pigment component.

In this study, peptoids (or *N*-substituted glycine oligomers) were used as a scaffold to display flavone and porphyrin in a face-to-face arrangement. Upon the incorporation of chiral aromatic side chains, the peptoid folds into a stable poly-proline type I (PPI) like helix, which has a pitch length of ~6.0 Å and periodicity of three residues per turn.[26] Structural investigations have elucidated several parameters (e.g., chain length or monomer composition) that affect the helical conformation.[27–32] Peptoids have also been shown to form other types of secondary structure, such as a peptoid ribbon structure,[33] and most notably, a threaded-loop conformation reported for peptoid nonamers in aprotic solvents.[34]

In previous work, we have exploited the unique structural properties of peptoids to construct porphyrin-peptoid conjugates (PPCs) displaying two or three porphyrins on the peptoid helix.[35–38] Initially, two tetraphenylporphyrins (TPPs) were displayed at different positions on the peptoid helix using a diaminobutane linkage between porphyrin and peptoid backbone, which provided a precise control over the spatial arrangement of the two porphyrins.[35] By switching one TPP to Zn-TPP, the energy transfer efficiency from the donor (i.e., Zn-TPP) to acceptor (i.e., free base TPP) was modulated with great precision by controlling the relative inter-porphyrin distance and orientation.[36] The conformational heterogeneity of the PPC was minimized by replacing the flexible *n*-butyl linkage with a more rigid phenyl linker to anchor the pigment to the peptoid backbone. Subsequently, enhanced control over the characteristic porphyrin interactions via intermolecular J-aggregation or intramolecular excitonic coupling

was achieved.[37] Thereafter, the potential application of the PPC was demonstrated in host-guest interactions and chiral recognition.[38]

During our continued efforts to construct peptoid-based artificial light-harvesting protein mimics using photosynthetic pigments, we noticed that the flavonoids have been less studied when compared to the porphyrins despite their unique photophysical properties. As mentioned above, flavone-porphyrin conjugates have been previously reported; however, flavone itself without any –OH or –OMe substituents is weakly fluorescent and less efficient for light-harvesting applications.[39] In the present study, we have developed an efficient synthetic route to prepare 4'-derivatized 7-methoxyflavone (7-MF, **3** and **4**, shown in Scheme 1) and successfully conjugated the pigment onto a peptoid scaffold using Miyaura borylation on a resin-bound peptoid followed by a Suzuki cross-coupling reaction. Unlike the parent (unsubstituted) flavone, the emission region of 7-MF (400−450 nm) overlaps with the maximum absorption wavelength of porphyrin (400−430 nm) making energy transfer between the two pigments feasible. The structural and photophysical properties of the flavone-porphyrin-peptoid conjugate (FPPC) were investigated using circular dichroism (CD), UV-vis, and fluorescence spectroscopies. Our donor-acceptor dyad represents a unique energy transfer system employing two important photosynthetic pigments, flavonoid and porphyrin, and potentially provides a model system to better understand the photophysical events occurring in natural photosynthesis.

Results and Discussion

Synthesis of the flavones

A Bpin-containing flavone derivative, 4'-(pinacolboryl)-7-methoxyflavone (**4**, 7-MF-Bpin), was synthesized from resacetophenone over four steps (Scheme 1). The two phenolic hydroxyl

groups of resacetophenone were initially protected as methyl ether upon reaction with MeI.[40] Then, the resulting methyl ketone (**1**) underwent a Claisen condensation with methyl 4-bromobenzoate to produce 1,3-diketone **2**, which contains an aryl bromide moiety. Subsequently, the flavone backbone was constructed via demethylative cyclization upon treatment with HBr (aq) and NaI in AcOH.[41] Gratifyingly, the unwanted demethylation of the *para*-methoxy group did not take place. It is proposed that the *ortho*-methoxy group is preferentially protonated via the assistance of the neighboring ketone moiety, thus resulting in the selective mono-demethylation reaction. Finally, the Miyaura borylation of aryl bromide **3** with B_2pin_2 afforded the desired product (**4**).[42] The overall yields of 7-MF-Br (**3**) and 7-MF-Bpin (**4**) were 33 and 16%, respectively.

Synthesis of the flavone-porphyrin-peptoid conjugate (FPPC)

Table 1. The sequences and structures of peptoids **5**–**8**.

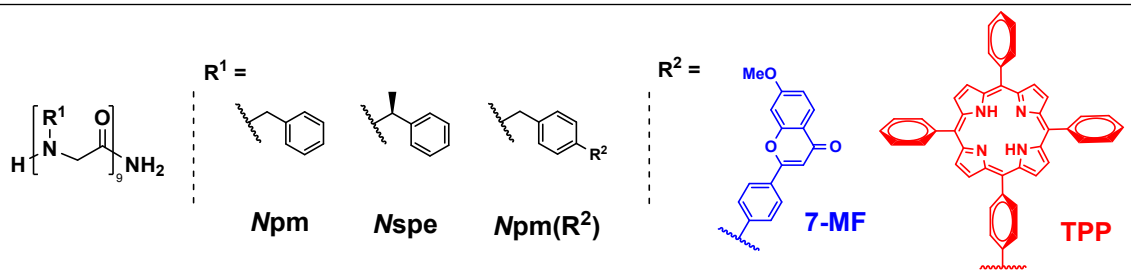

Compound	Sequence
5	H-*N*spe-*N*spe-*N*spe-*N*pm(TPP)-*N*spe-*N*spe-*N*pm(7-MF)-*N*spe-*N*spe-NH_2
6	H-*N*spe-*N*spe-*N*spe-*N*pm-*N*spe-*N*spe- *N*pm(7-MF)-*N*spe-*N*spe-NH_2
7	H-*N*spe-*N*spe-*N*spe-*N*pm-*N*spe-*N*spe-*N*pm(TPP)-*N*spe-*N*spe-NH_2
8	H-*N*pm-*N*pm-*N*pm-*N*pm(TPP)-*N*pm-*N*pm- *N*pm(7-MF)-*N*pm-*N*pm-NH_2

As shown in Table 1, peptoid nonamers **5**–**8** were designed to have a direct C-C linkage between the peptoid and pigment. Peptoid **5** is composed of a chiral submonomer ((*S*)-(–)-1-phenylethylamine, *N*spe) except at the positions of pigment conjugation, and a right-handed helical fold is expected.[26] The pigments were incorporated at the 3rd and 6th positions from the *C*-terminus, so the two pigments are at *i* and *i*+3 and spatially co-facial.[37] Control peptoids

6 and **7**, which contain only 7-MF or TPP, respectively, were prepared. Peptoid **8**, a non-helical version of **5**, was synthesized using an achiral monomer (benzylamine, *N*pm). The synthesis of the conjugates was achieved by repeating two processes: peptoid chain elongation and pigment conjugation (Scheme 2). For the synthesis of **5**, the peptoid pentamer containing one *para*-iodophenyl side chain was prepared via a solid-phase submonomer protocol (Scheme 2(a)).[43] Subsequently, the Miyaura borylation reaction of the aryl iodide on the resin-bound peptoid gave the Bpin-functionalized peptoid (Scheme 2(b) and 2(c)).[44] In our hands, the reaction was successfully carried out in DMF, but not in DMSO (data not shown). The overall conversion was calculated to be 70% from the iodophenyl peptoid using analytical HPLC (Figure S1). 7-MF-Br (**3**) was conjugated to the Bpin functionalized peptoid via a Suzuki-Miyaura cross-coupling reaction using the previously optimized conditions.[37] The peptoid was elongated to the desired chain length, and a cross-coupling reaction between TPP-Bpin and the iodophenyl side chain was carried out to yield the desired peptoid (**5**). Employing the same cross-coupling conditions, peptoids **6** and **7** were prepared using 7-MF-Bpin (**4**) and TPP-Bpin, respectively. All the conjugates were purified by preparative HPLC (>97%) and characterized using ESI-HRMS (Figure S2–6).

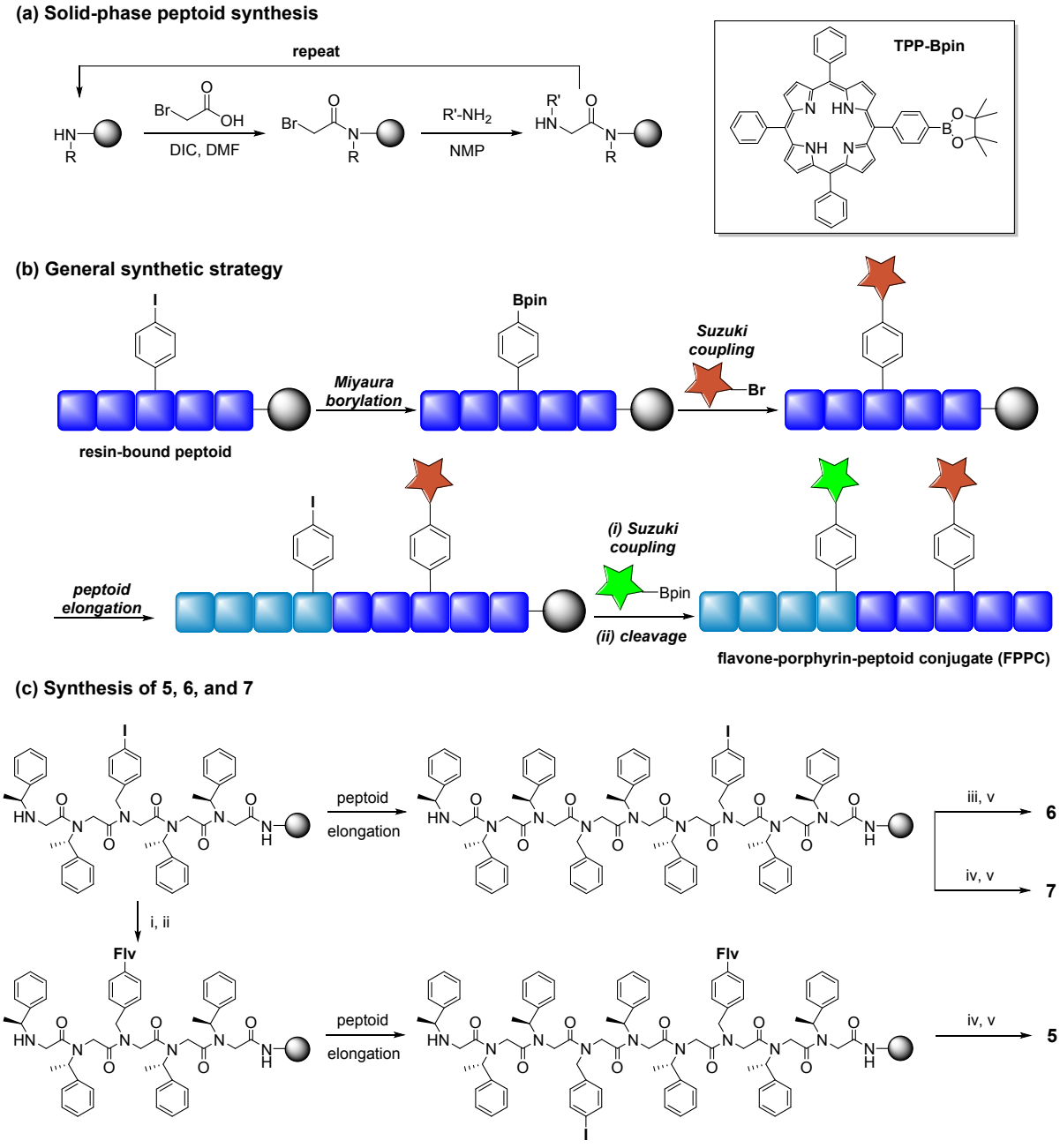

Scheme 2. (a) Peptoid submonomer synthesis. (b) Schematic representation of the general synthetic strategy used to prepare the FPPC. (c) Synthesis of **5**, **6**, and **7**. Reaction conditions: (i) B_2pin_2, $PdCl_2(dppf)$, dppf, KOAc, DMF, 80 °C, 24 h. (ii)−(iv) Pigment, $Pd(PPh_3)_4$, SPhos, K_2CO_3 (aq), DMF, H_2O, microwave irradiation, 80 °C, 3 h (pigment: (ii) **3**, (iii) **4**, and (iv) TPP-Bpin). (v) 50% TFA in CH_2Cl_2 (v/v), rt, 30 min.

Spectroscopic analysis of the peptoid conjugates

Peptoid oligomers composed of α-chiral side chains (e.g., *N*spe) typically exhibit helical secondary structures.[26] However, nonameric peptoids can adopt two distinct conformations, namely a helix or threaded-loop conformation, depending on the solvent used.[34] In aprotic solvents (e.g., MeCN), intramolecular hydrogen bonds formed between the *N*-terminal cationic ammonium and backbone carbonyl groups promote the formation of a threaded-loop conformation, while in protic media (e.g., MeCN/MeOH (1:1, v/v)), the peptoid converts back to its helical conformation. The circular dichroism (CD) spectra recorded for peptoids **5**–**7** in these two solvents demonstrate the conformational behavior of the peptoid nonamers (Figure 1). In MeCN, the increased negative ellipticity at 202 nm indicates a greater population of threaded-loop peptoids (Figure 1(a)), but in the presence of a protic solvent, the peptoids mainly show a helical CD signature with an intense *cis*-amide conformer peak at 220 nm (Figure 1(b)). The overall CD intensity observed for peptoids **5**–**7** confirms that the peptoid backbone was well-folded after the pigment conjugation step.[37] As expected, peptoid **8** was CD-silent in both solvents studied.

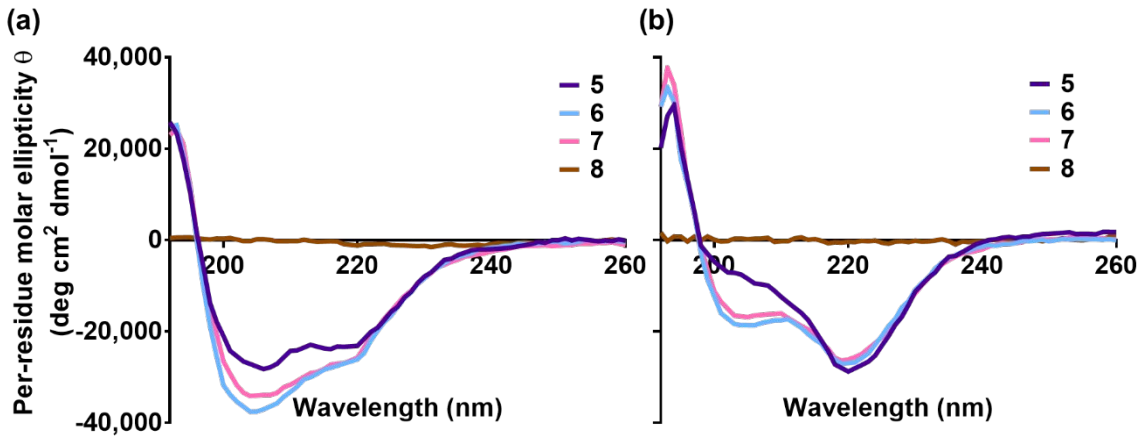

Figure 1. Circular dichroism (CD) spectra obtained for peptoids **5**–**8** (50 μM, 20 °C) recorded in (a) MeCN and (b) MeCN/MeOH (1:1, v/v).

UV-vis spectroscopy was used to characterize the pigments displayed on the peptoid in the range of 200–700 nm (Figure 2). Peptoids **6** and **7** show similar absorption spectra when compared to 7-MF (λ_{max} = 309 nm) or TPP (λ_{max} = 413 nm) (Figure S7) except for the strong peak observed at ~200 nm corresponding to the absorption of the aromatic side chains in the peptoid. The helical FPPC (**5**) exhibits characteristic peaks from both 7-MF and TPP. The absorption peaks observed for **5** are approximately the sum of the peaks of **6** and **7** without the appearance of a new peak or any peak shift. This indicates that the coupling between the ground state orbitals of 7-MF and TPP in **5** is negligible even when the two pigments are conjugated together on the peptoid. 7-MF displayed on helical peptoids **5** and **6** clearly shows a characteristic absorption at λ_{max} = 315 nm.[15] However, this peak was diminished when 7-MF was conjugated to non-helical peptoid **8**. Considering the poor solubility of **8** in both of the solvent systems studied, it was speculated that the non-specific aggregation of **8** affects the weak and broadened peak at ~327 nm. In helical peptoids **5** and **7**, the characteristic porphyrin absorption peaks can also be clearly identified.[37] In both MeCN and MeCN/MeOH, a sharp Soret band (λ_{max} = 414 nm) and four distinctive Q-bands (480–700 nm) were observed. In our previous study, a peptoid helix with a face-to-face display of two porphyrins showed dramatic porphyrin J-aggregation.[35,37] However, in **5** and **7**, neither the appearance of a red-shifted Soret band or a change in the Q-band intensity was observed, indicating the absence of porphyrin J-aggregation. Again, non-helical peptoid **8** showed diminished porphyrin Soret band and Q-bands. By comparing the UV-vis spectra of **5** and **8**, we confirmed that the helical structure of the peptoid scaffold is important to keep the pigments soluble in the polar media and to maintain the individual photophysical properties (e.g., extinction coefficient) of the conjugated pigments.

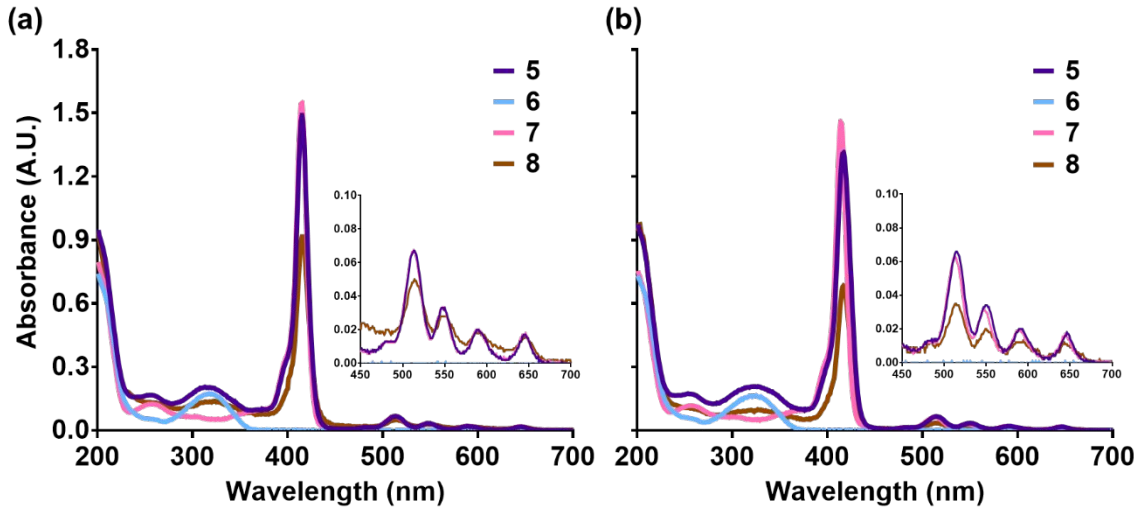

Figure 2. UV-vis absorption spectra obtained for peptoids **5**–**8** (50 μM, 20 °C) recorded in (a) MeCN and (b) MeCN/MeOH (1:1, v/v). The insets show the Q-band absorption region (450–700 nm).

Energy transfer in the FPPC

Fluorescence emission spectroscopy was used to investigate the energy transfer from 7-MF to TPP. Figures 3(a) and (b) show the emission spectra of **5**–**8** recorded in MeCN and MeCN/MeOH (1:1, v/v), respectively at the same concentration (5 μM). The excitation wavelength was 310 nm at which 7-MF is dominantly excited. The 7-MF emission of **6** occurs at 402 nm in MeCN and at 423 nm in MeCN/MeOH (1:1, v/v); the red-shift in the 7-MF emission observed in the latter can be explained by the hydrogen bonding between 7-MF and MeOH, which stabilizes the excited 7-MF species.[45] As shown in Figure 2, TPP has a minor absorption at 310 nm, resulting in the two emission bands of **7** observed between 630 nm and 750 nm in both of the solvent systems studied.

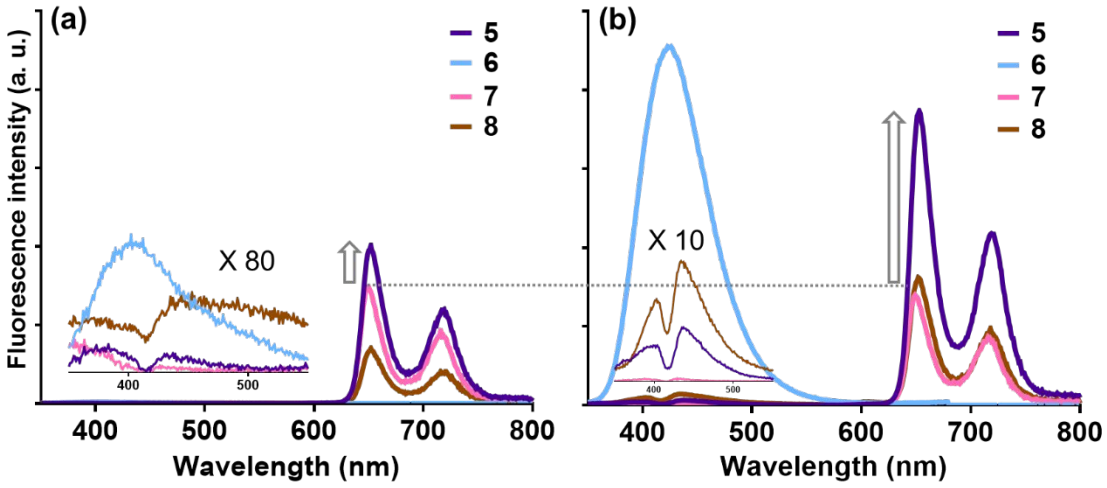

Figure 3. Fluorescence emission spectra of peptoids **5**–**8** (5 μM) recorded under the specific excitation wavelength of 7-MF (λ_{ex} = 310 nm) in (a) MeCN and (b) MeCN /MeOH (1:1, v/v). The insets show the magnified spectra around the 7-MF emission region. In (a), **5**–**8** are magnified 80 times. In (b), **5**, **7**, and **8** are magnified 10 times.

Quantitative analysis of the emission spectra can provide useful information regarding the energy transfer from 7-MF to TPP. For peptoids conjugated with a single pigment (**6** and **7**), the emissive process occurs without energy transfer from 7-MF to TPP, whereas the emission spectra of FPPC **5** includes the emissive process of the displayed pigments with energy transfer. When peptoid scaffold is in the helical conformation (Figure 3(b)), the TPP emission in **5** is strongly enhanced compared to that in **7** (shown by the gray arrow), while the 7-MF emission in **5** is drastically diminished compared to that in **6**. For the threaded-loop conformer (Figure 3(a)), similar trends of spectral change, but with much smaller magnitudes, were observed. Based on the absolute areas of the emission bands, the extents to which the TPP emission was enhanced and the 7-MF emission was decreased were compared (Table S1 and S2); the energy transfer from 7-MF to TPP is clearly more efficient when the peptoid is in a helical conformation. The energy transfer can be attributed to Förster resonance energy transfer

(FRET) facilitated by the short distance between 7-MF and TPP, and the spectral overlap of the donor emission and acceptor absorption (Figure S8).[46] This explanation was also supported by the valley observed at 414 nm in the 7-MF emission band of **5** (Figure 3, inset). This wavelength corresponds to the Soret band of TPP shown in Figure 2. Under both solvent conditions, unstructured FPPC **8** showed no clear evidence of energy transfer compared to that shown by **5**, demonstrating the importance of the spatially controlled orientation of the donor and acceptor pigments. We also examined the effect of photoexcitation at 550 nm with which only TPP can be excited and found no change in the emission bands observed for **5** and **7**, which indicates energy transfer does not occur in the reverse direction from TPP to 7-MF (Figure S9).

Energy transfer in **5** is more efficient in MeCN/MeOH than in MeCN, which reflects the effect of the peptoid backbone structure holding the donor and acceptor. In MeCN/MeOH, 7-MF and TPP in **5** are arranged in a co-facial manner on the well-defined helical peptoid with an inter-pigment distance of ~6 Å.[36] The increased population of threaded-loop conformers in MeCN results in the separation between 7-MF and TPP becoming larger (~14 Å).[34] In addition, the strongly enhanced 7-MF emission observed in MeCN/MeOH should be taken into account (**6** in Figure 3(b)). To confirm the effect of MeOH on the unusual enhancement of the 7-MF emission, we measured the fluorescence emission spectrum in a binary solvent system consisting of MeCN/MeOH with an increasing MeOH content (Figure S10). When the MeOH content was increased from 1 to 99%, the 7-MF emission peak area increased ~170-fold for **6** (Figure S11). However, this enhancement was much smaller for 7-MF alone (13-fold increment in the peak area). The enhancement in the emission of 7-MF in **6** was attributed to the protic solvent effect, which can restrict the degree of freedom of the molecular geometry of 7-MF; the direct C-C bond between 7-MF and the peptoid aromatic side chain or hydrophobic environment provided by helical peptoid backbone may play a role in this observation.[47–49]

However, further in-depth studies are warranted to explain this unexpected emission enhancement.

Conclusion

In summary, we have developed a synthetic route for the preparation of a flavone-porphyrin-peptoid conjugate (FPPC) as a novel artificial light-harvesting complex. An efficient synthesis of 4'-derivatized 7-methoxyflavone (7-MF-Bpin or 7-MF-Br) and the subsequent conjugation of 7-MF on a resin-bound peptoid using a Miyaura borylation followed by Suzuki cross-coupling reaction have been accomplished. Our optimized methods broaden the scope of the direct C-C bond forming conjugation reactions that can be applied to peptoids; any peptoid containing an aryl halide side chain can be converted into a peptoid containing the Bpin functionality, which can be used as a conjugation site to attach a variety of aryl halides (e.g., 7-MF-Br).

The helical structure of the peptoid scaffold was important in (1) keeping the hydrophobic pigments soluble in a polar medium and (2) maintaining the individual photophysical properties of each conjugated pigment. The steady-state fluorescence spectra indicate that characteristic intramolecular energy transfer occurs from the 7-MF donor to the porphyrin acceptor, transferring the absorbed UV energy into a visible light emission. The energy transfer efficiency was greater in the helix than that in the loop conformation of the peptoid. Our results demonstrate that helical peptoids provide excellent scaffolds for directing the interactions between the displayed pigments and can tailor their photophysical properties. Employing our synthetic pathway, it is possible to design more elaborate pigment-peptoid conjugates as efficient organic light-harvesting molecular machines with functional properties overcoming the weaknesses of natural systems.

Experimental Section

General information

Reactions were performed in oven-dried (140 °C) or flame-dried glassware under an atmosphere of dry argon unless otherwise noted. Tetrahydrofuran (THF, Fisher, HPLC grade) and 1,4-dioxane (Fisher, HPLC grade) were dried by percolation through a column packed with neutral alumina and a column packed with Q5 reactant, a supported copper catalyst for scavenging oxygen, under a positive pressure of argon. Acetone (Daejung) was distilled from $MgSO_4$ under argon, and acetic acid (Daejung) was distilled without a drying agent under argon prior to use. Solvents for recrystallization, work-up, and chromatography were hexanes (Duksan, Extra Pure), CH_2Cl_2 (Daejung, Extra Pure), Et_2O (Daejung, Extra Pure), EtOAc (Daejung, Extra Pure), and MeOH (Daejung, Extra Pure). Filtration and column chromatography were performed using Merck silica gel (SiO_2) 60 Å (0.040–0.063 mm). For reactions carried out above room temperature, oil bath was used as a heat source.

MeI (Alfa), K_2CO_3 (Duksan), NaHMDS (Alfa), HBr (aq. 48% (w/w), Daejung), NaI (Samchun), B_2pin_2 (Alfa), $PdCl_2$(dppf) (BePharm), KOAc (Duksan), Fmoc-Rink Amide MBHA resin (100–200 mesh, 0.65 mmol/g, Merck Millipore), and *N*,*N*′-diisopropylcarbodiimide (DIC, Advanced ChemTech) were used as received. For peptoid synthesis and Suzuki coupling reactions, peptide synthesis grade *N*,*N*-dimethylformamide (DMF; 99.8%) was used. The following reagents were recrystallized from the indicated solvent: resacetophenone (Alfa, CH_2Cl_2/hexanes) and methyl 4-bromobenzoate (Alfa, MeOH).

^{1}H NMR and ^{13}C{^{1}H} NMR spectra were recorded on a Jeol ECS400 (400 MHz/^{1}H, 100 MHz/^{13}C{^{1}H}) spectrometer. ^{1}H NMR and ^{13}C{^{1}H} NMR spectra were referenced to residual chloroform (7.26 ppm, ^{1}H, 77.23 ppm, ^{13}C{^{1}H}). Chemical shifts are reported in ppm, and

multiplicities are indicated by s (singlet), d (doublet), t (triplet), q (quartet), bs (broad singlet), and m (multiplet). Coupling constants, *J*, are reported in Hertz. Analytical thin-layer chromatography (TLC) was conducted on Merck silica gel 60 F_{254} TLC plates. Visualization was accomplished with UV (254 nm), $KMnO_4$, and *p*-anisaldehyde staining solution. High resolution electrospray ionization mass spectrometry (ESI-HRMS) was performed on an Agilent 6520 quadrupole-time-of-flight (Q-TOF) spectrometer. Data are reported in the form of (m/z).

Synthetic procedure for 1–4

Compound ***1***.[40, 50] 2',4'-dimethoxyacetophenone; To a stirred mixture of resacetophenone (1.5 g, 10 mmol) and dry K_2CO_3 (76 g, 550 mmol, 55 equiv) in acetone (15 mL) was added MeI (15 mL, 240 mmol, 24 equiv) at room temperature under Ar, and the mixture was refluxed. After 44 h, the reaction mixture was cooled to room temperature, diluted with CH_2Cl_2, and filtered through a glass frit. The filter cake was rinsed with CH_2Cl_2. The filtrate was concentrated under reduced pressure. The residue was diluted with EtOAc and washed with water. The aqueous layer was extracted with EtOAc twice. The combined organic layers were dried over $MgSO_4$, filtered through a glass frit, and concentrated under reduced pressure to give brownish orange solid. The crude material was purified by column chromatography (SiO_2, ϕ: 4.5 cm, *l*: 13 cm, EtOAc:hexanes = 1:6, R_f = 0.3, UV 254 nm) to afford **1** in 94% yield as off-white solid (1.7 g, 9.4 mmol). ^{1}H-NMR (400 MHz, $CDCl_3$): δ 7.83 (d, *J* = 8.9, 1H), 6.52 (dd, *J* = 8.7, 2.3, 1H), 6.46 (d, *J* = 2.4, 1H), 3.89 (s, 3H), 3.86 (s, 3H), 2.58 (s, 3H). ^{13}C{^{1}H}-NMR (100 MHz, $CDCl_3$): δ 198.0, 164.7, 161.3, 132.9, 121.4, 105.2, 98.5, 55.75, 55.66, 32.1.

Compound ***2***. 1-(4-bromophenyl)-3-(2,4-dimethoxyphenyl)-1,3-propanedione; To a stirred solution of **1** (2.0 g, 11 mmol) and methyl 4-bromobenzoate (2.6 g, 12 mmol, 1.1 equiv) in

THF (20 mL) was added a solution of NaHMDS (4.2 g, 23 mmol, 2.1 equiv) in THF (20 mL) at room temperature under Ar, and the flask was rinsed with THF (20 mL) twice. After 19 hours, the reaction mixture was partially concentrated under reduced pressure, diluted with Et_2O, and acidified until pH = 3 with aq 1 N HCl. The organic layer was separated, and the aqueous layer was extracted with Et_2O twice. The combined organic layers were dried over $MgSO_4$, filtered through a glass frit, and concentrated under reduced pressure to give orange solid. The crude material was purified by column chromatography (SiO_2, ϕ: 3 cm, l: 14 cm, CH_2Cl_2, R_f = 0.6, UV 254 nm) and recrystallized from EtOAc/hexanes to afford **2** in 63% yield as yellow fibers (2.5 g, 6.9 mmol). m. p.: 133.6-134.7 ℃. ^{1}H-NMR (400 MHz, $CDCl_3$): δ 17.06 (bs, 1H), 8.00-7.97 (m, 1H), 7.80-7.78 (m, 2H), 7.60-7.57 (m, 2H), 7.13 (s, 1H), 6.58 (dd, J = 8.7, 2.3, 1H), 6.48 (d, J = 2.3, 1H), 3.93 (s, 3H), 3.86 (s, 3H). ^{13}C{^{1}H}-NMR (100 MHz, $CDCl_3$): δ 184.01, 183.96, 164.4, 160.7, 135.2, 132.4, 131.9, 128.7, 126.8, 117.5, 105.5, 98.8, 97.6, 55.9, 55.7. HRMS (ESI): m/z: calcd for $C_{17}H_{16}{}^{79}BrO_4$ $[M + H]^+$, $C_{17}H_{16}{}^{81}BrO_4$ $[M + H]^+$: 363.0232, 365.0212, found 363.0214, 365.0185.

*Compound **3**.*[41, 51] 4'-bromo-7-methoxyflavone; To a stirred solution of **2** (2.2 g, 6.0 mmol) and NaI (4.5 g, 30 mmol, 5.0 equiv) in AcOH (34 mL, 590 mmol, 99 equiv) was added 48% (w/w) aq HBr (14 mL, 120 mmol, 20 equiv) at room temperature under Ar, and the mixture was heated to 80 ℃. After 17 h, the reaction mixture was cooled to room temperature and poured to anhydrous K_2CO_3 (100 g). The mixture was diluted with water and extracted with Et_2O. The aqueous layer was extracted with EtOAc three times. The combined organic layers were washed with sat. aq $NaHSO_3$, dried over $MgSO_4$, and filtered through a glass frit. The filter cake was rinsed with CH_2Cl_2. The filtrate was concentrated under reduced pressure to give pink solid. The crude material was purified by column chromatography (SiO_2, ϕ: 3 cm, l: 12.5 cm, loading: CH_2Cl_2, elution: EtOAc:hexanes = 2:5, R_f = 0.2, UV 254 nm) and recrystallized from

EtOAc to afford **3** in 55% yield as pink crystals (1.1 g, 3.3 mmol). m. p.: 181.3-182.6 ℃. ^{1}H-NMR (400 MHz, $CDCl_3$): δ 8.08 (d, J = 8.9, 1H), 7.73 (m, 2H), 7.62 (m, 2H), 6.96 (dd, J = 8.9, 2.4, 1H), 6.92 (d, J = 2.4, 1H), 6.72 (s, 1H), 3.91 (s, 3H). ^{13}C{^{1}H}-NMR (100 MHz, $CDCl_3$): δ 177.8, 164.5, 162.1, 158.0, 132.4, 130.8, 127.7, 127.2, 126.3, 117.8, 114.8, 107.7, 100.5, 56.1. HRMS (ESI): m/z: calcd for $C_{16}H_{12}{}^{79}BrO_3$ $[M + H]^+$, $C_{16}H_{12}{}^{81}BrO_3$ $[M + H]^+$: 330.9970, 332.9949, found 330.9960, 332.9937.

*Compound **4**.*[42] 4'-(pinacolboryl)-7-methoxyflavone; A stirred mixture of **3** (0.33 g, 1.0 mmol), B_2pin_2 (0.51 g, 2.0 mmol, 2.0 equiv), $PdCl_2$(dppf) (37 mg, 0.051 mmol, 5 mol%), and KOAc (0.39 g, 4.0 mmol, 4.0 equiv) in degassed 1,4-dioxane (4 mL) was heated to 85 ℃ under Ar. After 44 hours, the reaction mixture was cooled to room temperature and concentrated under reduced pressure. The residue was diluted with CH_2Cl_2 and washed with sat. aq $NaHCO_3$. The aqueous layer was extracted CH_2Cl_2 three times. The combined organic layers were dried over $MgSO_4$, filtered through a glass frit, and concentrated under reduced pressure to give pale brown solid. Because **4** is somewhat unstable on SiO_2, the crude material was quickly filtered through SiO_2 (ϕ: 4 cm, l: 7 cm, EtOAc, R_f = 0.9, UV 254 nm) and precipitated from CH_2Cl_2/hexanes to afford **4** in 50% yield as off-white powder (189 mg, 0.500 mmol). ^{1}H-NMR (400 MHz, $CDCl_3$): δ 8.12-8.10 (m, 1H), 7.94-7.87 (m, 4H), 6.99-6.96 (m, 2H), 6.82 (s, 1H), 3.92 (s, 3H), 1.36 (s, 12H). ^{13}C{^{1}H}-NMR (100 MHz, $CDCl_3$): δ 178.0, 164.5, 163.1, 158.2, 135.4, 134.2, 132.6, 127.2, 125.4, 117.9, 114.9, 108.0, 100.5, 84.4, 56.1, 25.1. HRMS (ESI): m/z: calcd for $C_{22}H_{24}BO_5$ $[M + H]^+$: 379.1717, found 379.1723.

Synthetic procedure for peptoids 5–8

Peptoid synthesis protocol. Peptoids were synthesized by the microwave-assisted solid-phase submonomer synthesis method.[43] The reactions were run in a cartridge (Applied Separations,

Allentown, PA, USA, 25 mL) assembled with a filter (Applied Separations, 20 micron) and accelerated by a CEM MARS 230/60 microwave reaction system (CEM Corp., Matthews, NC, USA) using a fiber optic temperature probe and magnetic stirrer under atmospheric pressure. The resin (0.25 mmol, 0.48 g) was swelled in DMF for 20 min and was treated twice with 20% (v/v) piperidine in DMF (5 min and 20 min, 10 mL each) for Fmoc deprotection. Bromoacetylation was performed by the addition of bromoacetic acid (6.25 mmol, 1.2 M in DMF, 5.21 mL) and DIC (5.63 mmol, 0.87 mL). The mixture was stirred in a microwave oven (300 W max power, 35 °C, ramp 30 s) for 1 min and washed with CH_2Cl_2 and DMF. Amine displacement was carried out by the addition of (*S*)-(-)-α-methylbenzylamine (*N*spe, 3.75 mmol, 1.0 M in NMP, 3.75 mL), benzylamine (*N*pm, 3.75 mmol, 1.0 M in NMP, 3.75 mL), or 4-iodobenzylamine (*N*pib, 3.75 mmol, 1.0 M in NMP, 3.75 mL) to the bromoacetylated peptoids. The mixture was stirred in a microwave oven (300 W max power, 80 °C, ramp 2 min) for 90 s and washed with CH_2Cl_2 and DMF. Bromoacetylation and amine displacement were repeated until the desired sequence was obtained. Peptoids were cleaved from the resin with 50:50 (v/v) TFA/ for 30 minutes at room temperature. The cleavage reaction solution was filtered by solid-phase extraction (SPE) cartridges with 20 μ PE frit (Applied Separations, Allentown, PA, USA), and the volatiles were removed by a stream of nitrogen. The crude peptoid was dissolved in MeCN and analyzed by ESI-MS and analytical HPLC as described below.

Synthesis of resin-bound peptoid-boronic acid pinacol ester. The resin-bound iodophenyl-containing peptoids (0.125 mmol) were suspended in CH_2Cl_2 for 20 min, and the solvent was drained. Miyaura borylation reactions were conducted by the addition of bis(pinacolato)diboron (B_2pin_2; 127.0 mg, 0.500 mmol), 1,1'-ferrocenediyl-bis(diphenylphosphine) (dppf; 6.2 mg, 0.011 mmol), Pd(dppf)Cl_2 (16.5 mg, 0.023 mmol), and

a sonicated solution of potassium acetate in degassed DMF (0.2 M, 3.75 mL). The mixture was stirred for 24 h at 80 °C. The resin was washed with CH_2Cl_2 and DMF.

General conditions for Suzuki-Miyaura cross-coupling reactions on-resin. The resin-bound peptoids (0.019 mmol) were suspended in CH_2Cl_2 for 20 min, and the solvent was drained. To the resin was added **4** (35.9 mg, 0.095 mmol) or TPP-Bpin[37] (70.4 mg, 0.095 mmol), $Pd(PPh_3)_4$ (6.5 mg, 0.006 mmol), 2-dicyclohexylphosphino-2',6'-dimethoxybiphenyl (SPhos; 12.8 mg, 0.011 mmol), and DMF (2.0 mL), and aqueous potassium carbonate solution (1.3 M, 0.07 mL) was added to initiate the reaction. The mixture was stirred for 3 h at 80 °C (microwave open, 300 W, opened in the air, ramp 2 min). The resin was successively washed with CH_2Cl_2 and DMF.

HPLC purification. Analytical HPLC was conducted using a Waters reversed-phase HPLC system (Waters 2489 UV/visible detector, Waters 1525 Binary HPLC pump, Waters 2707 Autosampler, and Waters 5CH column oven) on a C18 column (SunFire C18, 4.6 × 250 mm, 5 μm) at 40 °C. A binary mobile phase system (A: deionized water + 0.1% TFA, B: MeCN + 0.1% TFA) was employed as follows: 5 min 30% of B, a linear gradient to 100% of B during 15 min, and then holding 100% of B for 13 min. The flow rate was 1 mL/min. The purity of the compound was monitored by measuring absorbance at 220 nm. All the peptoids were purified on a Waters preparative HPLC system (Waters 2489 UV/visible detector, Waters 2545 Quaternary HPLC pump, Waters fraction collector III) with a C18 column (SunFire C18, 19 x 150 mm, 5 μm) at room temperature. The flow rate was set to 14 mL/min, and a binary mobile phase system (A: deionized water + 0.1% TFA, B: MeCN + 0.1% TFA) was used under the following conditions: 5 min 30% of B, a linear gradient to 100% B during 20 min, followed by 100% of B for 5 min. Sample elution was monitored by measuring the absorbance at 220 nm,

and the purity of each fraction (>97%) was confirmed by analytical HPLC. ESI-MS analysis was carried out on an Agilent 1260 Infinity liquid chromatography system with an Agilent 6120 single quadrupole mass spectrometer. Fractions containing the pure product were collected, lyophilized, and stored at −80 °C. The amount of purified peptoid and overall yield based on the resin loading are shown as follows: **5** (5.7 mg, 15%), HRMS (ESI): m/z: calcd for $C_{148}H_{136}N_{14}O_{12}$ $[M + H]^+$: 2301.0462, found 2302.0498. Purity according to analytical HPLC: 97%. **6** (5.7 mg, 17%), HRMS (ESI): m/z: calcd for $C_{104}H_{108}N_{10}O_{12}$ $[M + H]^+$: 1688.8148, found 1689.8207. Purity according to analytical HPLC: 99%. **7** (9.6 mg, 24%), HRMS (ESI): m/z: calcd for $C_{132}H_{126}N_{14}O_9$ $[M + H]^+$: 2050.9832, found 2051.9874. Purity according to analytical HPLC: 99%. **8** (0.5 mg, 3%), HRMS (ESI): m/z: calcd for $C_{141}H_{122}N_{14}O_{12}$ $[M + H]^+$: 2202.9367, found 2203.9365. Purity according to analytical HPLC: 97%.

Spectral analysis

CD spectra were recorded on a Jasco model 810 spectropolarimeter (Jasco, Easton, MD, USA) in a quartz cell with 1 mm path length. The response time was set to 1 second with 1.0 nm bandwidth for all spectra. The samples were prepared in either MeCN or MeOH, and the spectra were acquired in the 190−260 nm range with a 20 nm min^{-1} scanning speed at 20 °C. The spectra were measured three times and averaged. The results were expressed in terms of per-residue molar ellipticity, [θ] (deg cm^2 $dmol^{-1}$). ($[\theta] = \theta / (n \times c \times l)$, where θ = the ellipticity of the polarization, n = the number of amide groups present, c = the molar concentration, l = the optical path length).[26]

UV-vis spectra were recorded on an Ultrospec 2100 Pro UV-vis spectrophotometer (GE Healthcare, Buckinghamshire, UK) in the range of 200−700 nm, in a quartz cell with 1 mm path length at ambient temperature. Baseline correction for each spectrum was performed with blank solvent.

Fluorescence emission and excitation spectra were observed on an FLS980 fluorescence spectrometer (Edinburgh Instruments, Livingston, UK). All peptoids were prepared at concentration 5 μM with solvent MeCN or MeCN/MeOH (1:1, v/v). All spectra measurements were performed with Xe Lamp installed in FLS980 with excitation and emission spectral bandwith of 1 nm both, dwell time of 0.1 and repetition of 5 times. Fluorescence emission spectra of all samples were obtained with excitation wavelength at 310 nm and 550 nm. Fluorescence excitation spectra were performed at emission wavelength 425 nm for MeCN/MeOH (1:1, v/v) or 400 nm for MeCN and 650 nm for both solvents.

Associated content

Supporting Information.

The Supporting Information is available free of charge on the ACS Publication website at DOI: xxx/xxx.

^{1}H and $^{13}C\{^{1}H\}$ NMR spectra for **1**–**4**, HPLC data and ESI-HRMS (ToF) data for **5**–**8**, additional UV-vis absorption spectra and fluorescence emission spectra, and fluorescence photographs.

Acknowledgments

This work was financially supported by the National Research Foundation of Korea (NRF-2018R1A2B6007535 to J.S.) and by the Creative Materials Discovery Program (NRF-2018M3D1A1052659 to J.S.), which is funded by the National Research Foundation (NRF) under the Ministry of Science and ICT. H.L. and H.O. were supported by GIST Research Institute (GRI) grant funded by the GIST in 2019.

References

1. Blankenship, R. E. *Molecular mechanism of photosynthesis*. 2nd ed.; Wiley-Blackwell: Oxford, U.K., 2014.

2. Springer, J. W. P.-L., P. S.; Reddy, K. R.; Krayer, M.; Jiao, J.; Lee, G. M.; Niedzwiedzki, D. M.; Harris, M. A.; Kirmaier, C.; Bocian, D. F.; Lindsey, J. S.; Holten, D.; Loach, P. A. Biohybrid photosynthetic antenna complexes for enhanced light-harvesting. *J. Am. Chem. Soc.* **2012**, 134, 4589–4599.

3. Woller, J. G. H., J. K.; Albinsson B. Self-assembled nanoscale DNA-porphyrin complex for artificial light harvesting. *J. Am. Chem. Soc.* **2013**, 135, 2759–2768.

4. Gust, D. M., T. A.; Moore, A. L.; Devadoss, C.; Liddell, P. A.; Hermant, R.; Nieman, R. A.; Demanche, L. J.; DeGraziano, J. M.; Gouni, I. Triplet and singlet energy transfer in carotene-porphyrin dyads: role of the linkage bonds. *J. Am. Chem. Soc.* **1992**, 114, 3590–3603.

5. Sun, Y. G., F.; Zuo, T.; Hua, J.; Diao, G. Stimulus-responsive light-harvesting complexes based on the pillararene-induced co-assembly of b-carotene and chlorophyll. *Nat. Commun.* **2016**, 7, 12042.

6. Samanta, A.; Das, G.; Das, S. K. Roles of flavonoids in plants. *Int. J. Pharm. Sci. Tech.* **2011**, *6*, 12–35.

7. Clegg, M. T.; Durbin, M. L. Flower color variation: a model for the experimental study of evolution. *Proc. Natl. Acad. Sci. U.S.A.* **2000**, *97*, 7016–7023.

8. Agati, G.; Tattini, M. Multiple functional roles of flavonoids in photoprotection. *New Phytologist* **2010**, *186*, 786–793.

9. Vidovic, M.; Morina, F.; Milic, S.; Zechmann, B.; Albert, A.; Winkler, J. B.; Jovanovic, V. Ultraviolet-B component of sunlight stimulates photosynthesis and flavonoid accumulation in variegated *Plectranthus coleoides* leaves depending on background light. *Plant, Cell &*

Environ. **2015**, *38*, 968–979.

10. Fini, A.; Brunetti, C.; Ferdinando, M. D.; Ferrini, F.; Tattini, M. Stress-induced flavonoid biosynthesis and the antioxidant machinery of plants. *Plant Signal. Behav.* **2011**, *6*, 709–711.

11. Yamasaki, H.; Sakihama, Y.; Ikehara, N. Flavonoid-peroxidase reaction as a detoxification mechanism of plant cells against H_2O_2. *Plant Physiol.* **1997**, *115*, 1405–1412.

12. Peer, W. A.; Murphy, A. S. *Flavonoids as signal molecules: targets of flavonoid action*. Springer: New York, 2006; p 239–268.

13. Cushnie, T. P. T.; Lamb, A. J. Antimicrobial activity of flavonoids. *Int. J. Antimicrob. Agents* **2005**, *26*, 343–356.

14. Panche, A. N.; Diwan, A. D.; Chandra, S. R. Flavonoids: an overview. *J. Nut. Sci.* **2016**, *5*, 1–15.

15. Halbwirth, H. The creation and physiological relevance of divergent hydroxylation patterns in the flavonoid pathway. *Int. J. Mol. Sci.* **2010**, *11*, 595–621.

16. Chebil, L.; Humeau, C.; Anthoni, J.; Dehez, F.; Engasser, J.-M.; Ghoul, M. Solubility of flavonoids in organic solvents. *J. Chem. Eng. Data* **2007**, *52*, 1552–1556.

17. Marby, T. J.; Markham, K. R.; Thomas, M. B. *The systematic identification of flavonoids*. Springer-Verlag: Berlin-Heidelberg-New York, 1970; p 33–250.

18. Trouillas, P.; Sancho-Garcia, J. C.; De Freitas, V.; Gierschner, J.; Otyepka, M.; Dangles, O. Stabilizing and modulating color by copigmentation: insights from theory and experiment. *Chem. Rev.* **2016**, *116*, 4937–4982.

19. Yıldız, S. Z.; Küçükislamog˘lu, M.; Tuna, M. Synthesis and characterization of novel flavonoid-substituted phthalocyanines using (±)naringenin. *J. Organomet. Chem.* **2009**, *694*, 4152–4161.

20. Enes, R. F.; Farinha, A. S. F.; Tomé, A. C.; Cavaleiro, J. A. S.; Amorati, R.; Petrucci, S.; Pedulli, G. F. Synthesis and antioxidant activity of [60]fullerene-flavonoid conjugates.

Tetrahedron **2009**, *65*, 253–262.

21. Nakagawa-Goto, K.; Yamada, K.; Nakamura, S.; Chen, T.-H.; Chiang, P.-C.; Bastow, K. F.; Wang, S.-C.; Spohn, B.; Hung, M.-C.; Lee, F.-Y.; Lee, F.-C.; Lee, K.-H. Antitumor agents. 258. Syntheses and evaluation of dietary antioxidant—taxoid conjugates as novel cytotoxic agents. *Bioorg. Med. Chem. Lett.* **2007**, *17*, 5204–5209.

22. Sousa, R. M. S.; Pinto, D. C. G. A.; Silva, A. M. S.; Serra, V. V.; Barros, A. I. R. N. A.; Faustino, M. A. F.; Neves, M. G. P. M. S.; Cavaleiro, J. A. S. Flavone-nitrogen heterocycle conjugate formation by 1,3-dipolar cycloadditions. *Eur. J. Org. Chem.* **2012**, 132–143.

23. Lopes, S. P.; Menezes, J. C. J. M. D. S.; Hackbarth, S.; Pinto, D. C. G. A.; Faustino, M. A. F.; Silva, A. M. S.; Neves, M. G. P. M. S.; Roder, B.; Cavaleiro, J. A. S. New flavonoid-porphyrin conjugates via Buchwald-Hartwig amination: synthesis and photophysical studies. *Tetrahedron Lett.* **2013**, *54*, 5253–5256.

24. Mao, M.; Song, Q.-H. Non-conjugated dendrimers with a porphyrin core and coumarin chromophores as peripheral units: synthesis and photophysical properties. *Dyes Pigments* **2012**, *92*, 975–981.

25. Garg, V.; Kodis, G.; Liddell, P. A.; Terazono, Y.; Moore, T. A.; Moore, A. L.; Gust, D. Artificial photosynthetic reaction center with a coumarin-based antenna system. *J. Phys. Chem. B* **2013**, *117*, 11299–11308.

26. (a) Armand, P.; Kirshenbaum, K.; Falicov, A.; Dunbrack Jr, R. L.; Dill, K. A.; Zuckermann, R. N.; Cohen, F. E. Chiral N-substituted glycines can form stable helical conformations. *Fold. Des.* **1997**, *2*, 369–375. (b) Armand, P.; Kirshenbaum, K.; Goldsmith, R. A.; Farr-Jones, S.; Barron, A. E.; Truong, K. T. V.; Dill, K. A.; Mierke, D. F.; Cohen, F. E.; Zuckermann, R. N.; Bradley, E. K. NMR determination of the major solution conformation of a peptoid pentamer with chiral side chains. *Proc. Natl. Acad. Sci.* **1998**, *95*, 4309–4314. (c) Kirshenbaum, K.; Barron, A. E.; Goldsmith, R. A.; Armand, P.; Bradley, E. K.; Truong, K. T. V.; Dill, K. A.;

Cohen, F. E.; Zuckermann, R. N. Sequence-specific polypeptoids: a diverse family of heteropolymers with stable secondary structure. *Proc. Natl. Acad. Sci.* **1998**, *95*, 4303–4308.

27. Wu, C. W.; Sanborn, T. J.; Huang, K.; Zuckermann, R. N.; Barron, A. E. Peptoid oligomers with a-chiral, aromatic side chains: sequence requirements for the formation of stable peptoid helices. *J. Am. Chem. Soc.* **2001**, *123*, 6778–6784.

28. Stringer, J. R.; Crapster, J. A.; Guzei, I. A.; Blackwell, H. E. Extraordinarily robust polyproline type I peptoid helices generated via the incorporation of a-chiral aromatic *N*-1-Naphthylethyl side chains. *J. Am. Chem. Soc.* **2011**, *133*, 15559–15567.

29. Shin, H.-M.; Kang, C.-M.; Yoon, M.-H.; Seo, J. Peptoid helicity modulation: precise control of peptoid secondary structures via position-specific placement of chiral monomers. *Chem. Commun.* **2014**, *50*, 4465–4468.

30. Laursen, J. S.; Harris, P.; Fristrup, P.; Olsen, C. A. Triangular prism-shaped β-peptoid helices as unique biomimetic scaffolds. *Nat. Commun.* **2015**, *6*, 7013.

31. Wellhöfer, I.; Frydenvang, K.; Kotesova, S.; Christiansen, A. M.; Laursen, J. S.; Olsen, C. A. Functionalized helical β-peptoids. *J. Org. Chem.* **2019**, *84*, 3762–3779.

32. Gimenez, D.; Zhou, G.; Hurley, M. F. D.; Aguilar, J. A.; Voelz, V. A.; Cobb, S. L. Fluorinated aromatic monomers as building blocks to control α-peptoid conformation and structure. *J. Am. Chem. Soc.* **2019**, *141*, 3430–3434.

33. Crapster, J. A.; Guzei, I. A.; Blackwell, H. E. A peptoid ribbon secondary structure. *Angew. Chem. Int. Ed.* **2013**, *52*, 5079–5084.

34. Huang, K.; Wu, C. W.; Sanborn, T. J.; Patch, J. A.; Kirshenbaum, K.; Zuckermann, R. N.; Barron, A. E.; Radhakrishnan, I. A threaded loop conformation adopted by a family of peptoid nonamers. *J. Am. Chem. Soc.* **2006**, *128*, 1733–1738.

35. Kang, B.; Chung, S.; Ahn, Y. D.; Lee, J.; Seo, J. Porphyrin-peptoid conjugates: face-to-face display of porphyrins on peptoid helices. *Org. Lett.* **2013**, *15*, 1670–1673.

36. Kang, B.; Yang, W.; Lee, S.; Mukherjee, S.; Forstater, J.; Kim, H.; Goh, B.; Kim, T.-Y.; Voelz, V. A.; Pang, Y.; Seo, J. Precisely tuneable energy transfer system using peptoid helix-based molecular scaffold. *Sci. Rep.* **2017**, *7*, 4786.

37. Yang, W.; Kang, B.; Voelz, V. A.; Seo, J. Control of porphyrin interactions via structural changes of a peptoid scaffold. *Org. Biomol. Chem.* **2017**, *15*, 9670–9679.

38. Lee, Y. J.; Kang, B.; Seo, J. Metalloporphyrin dimers bridged by a peptoid helix: host-guest interaction and chiral recognition. *Molecules* **2018**, *23*, 2741.

39. (a) Schipfer, R.; Wolfbeis, O. S.; Knierzinger, A. pH-dependent fluorescence spectroscopy. Part 12. flavone, 7-hydroxyflavone, and 7-methoxyflavone. *J. C. S. Perkin II* **1981**, 1443–1448. (b) Christoff, M.; Toscano, V. G.; Baader, W. J. Influence of methoxy substitution on flavonoid photophysics: a steady state and laser flash photolysis study. *J. Photochem. Photobiol. A* **1996**, *101*, 11–20.

40. Khatib, S.; Nerya, O.; Musa, R.; Shmuel, M.; Tamir, S.; Vaya, J. Chalcones as potent tyrosinase inhibitors: the importance of a 2,4-substituted resorcinol moiety. *Bioorg. Med. Chem.* **2005**, *13*, 433–441.

41. (a) Lee, J. I.; Son, H. S.; Jung, M. G. A novel synthesis of flavones from 2-methoxybenzoic acids. *Bull. Korean Chem. Soc.* **2005**, *26*, 1461–1463. (b) Kawasaki, I.; Matsuda, K.; Kaneko, T. Preparation of 1,7-bis(p-hydroxyphenyl)heptane. *Bull. Chem. Soc. Jpn.* **1971**, *44*, 1986–1987.

42. Gu, B.; Wu, W.; Xu, G.; Feng, G.; Yin, F.; Chong, P. H. J.; Qu, J.; Yong, K.-T.; Liu, B. Precise two-photon photodynamic therapy using an efficient photosensitizer with aggregation-induced emission characteristics. *Adv. Mater.* **2017**, *29*, 1701076.

43. Zuckermann, R. N.; Kerr, J. M.; Kent, S. B. H.; Moos, W. H. Efficient method for the preparation of peptoids [oligo(N-substituted glycines)] by submonomer solid-phase synthesis. *J. Am. Chem. Soc.* **1992**, *114*, 10646–10647.

44. Afonso, A.; Roses, C.; Planas, M.; Feliu, L. Biaryl peptides from 4-iodophenylalanine by solid-phase borylation and Suzuki-Miyaura cross-coupling. *Eur. J. Org. Chem.* **2010**, *8*, 1461–1468.

45. Park, H.; Yu, D.; Park, J. K.; Bark, K. Spectroscopic properties of flavonoids in various aqueous-organic solvent mixtures. *Bull. Korean Chem. Soc.* **2013**, *34*, 211–220.

46. Turro, N. J.; Ramamurthy, V.; Scaiano, J. C. *Principles of Molecular Photochemistry: An Introduction*; 1st Ed. University Science Books: Sausalito-California, 2009; p 400–411.

47. Fuller, A. A.; Seidl, F. J.; Bruno, P. A.; Plescia, M. A.; Palla, K. S. Use of environmentally sensitive fluorophore 4-*N,N*-dimethylamino-1,8-naphthalimide to study peptoid helix structures. *Pep. Sci.* **2011**, *96*, 627–638.

48. Fuller, A. A.; Yurash, B. A.; Schaumann, E. N.; Seidl, F. J. Self-association of water-soluble peptoids comprising (*S*)-*N*-1-(naphthylethyl)glycine residues. *Org. Lett.* **2013**, *15*, 5118–5121.

49. Shi, Y.; Yin, G.; Yan, Z.; Sang, P.; Wang, M.; Brzozowski, R.; Eswara, P.; Wojtas, L.; Zheng, Y.; Li, X.; Cai, J. Helical sulfono-γ-AApeptides with aggregation-induced emission and circularly polarized luminescence. *J. Am. Chem. Soc.* **2019**, *141*, 12697–12706.

50. Lindh, J.; Sjöberg, P. J. R.; Larhed, M. Synthesis of aryl ketones by palladium(II)-catalyzed decarboxylative addition of benzoic acids to nitriles. *Angew. Chem. Int. Ed.* **2010**, *49*, 7733–7737.

51. Ghani, S. B. A.; Weaver, L.; Zidan, Z. H.; Ali, H. M.; Keevil, C. W.; Brown, R. C. D. Microwave-assisted synthesis and antimicrobial activities of flavonoid derivatives. *Bioorg. Med. Chem. Lett.* **2008**, *18*, 518–522.

TOC Figure

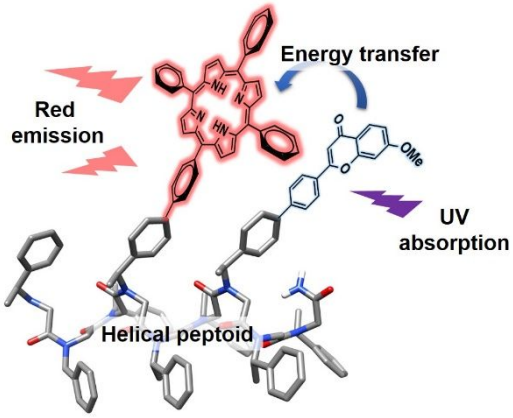
Energy transfer
Red
emission
OMe
UV
absorption
Helical peptoid